Award Number: W81XWH-20-1-0337

TITLE: In Vivo Validation of Cell of Origin and Candidate Drivers of Group 4 Medulloblastoma

PRINCIPAL INVESTIGATOR: Christin Schmidt

CONTRACTING ORGANIZATION: University of California, San Francisco, CA

REPORT DATE: December 2022

TYPE OF REPORT: Final

PREPARED FOR: U.S. Army Medical Research and Development Command
Fort Detrick, Maryland 21702-5012

REPORT DOCUMENTATION PAGE

Form Approved
OMB No. 0704-0188

1. REPORT DATE	2. REPORT TYPE	3. DATES COVERED
December 2022	Final	01Sep2020-31Aug2022

4. TITLE AND SUBTITLE

In Vivo Validation of Cell of Origin and Candidate Drivers of Group 4 Medulloblastoma

5a. CONTRACT NUMBER
W81XWH-20-1-0337

5b. GRANT NUMBER
CA191085

5c. PROGRAM ELEMENT NUMBER

6. AUTHOR(S)
Christin Schmidt

E-Mail: christin.schmidt@ucsf.edu

5d. PROJECT NUMBER

5e. TASK NUMBER

5f. WORK UNIT NUMBER

7. PERFORMING ORGANIZATION NAME(S) AND ADDRESS(ES)

The Regents of the University of California, San Francisco, 1855 Folsom Street, Ste. 425, San Francisco, CA 94143-4249

8. PERFORMING ORGANIZATION REPORT NUMBER

9. SPONSORING / MONITORING AGENCY NAME(S) AND ADDRESS(ES)

U.S. Army Medical Research and Development Command
Fort Detrick, Maryland 21702-5012

10. SPONSOR/MONITOR'S ACRONYM(S)

11. SPONSOR/MONITOR'S REPORT NUMBER(S)

12. DISTRIBUTION / AVAILABILITY STATEMENT

Approved for Public Release; Distribution Unlimited

13. SUPPLEMENTARY NOTES

14. ABSTRACT

Medulloblastoma is the most common childhood brain tumor and is a major cause of cancer related mortality in children. Although current treatment strategies reach a 60-80% 5-year survival rate, a proportion of cases remain unresponsive to therapy and lack more effective treatment options. A significant molecular heterogeneity exists within the medulloblastoma subgroups, especially within Group 4 medulloblastoma (G4-MB), challenging the choice and prediction of response to a particular therapy. Our objective is to define the cell-of-origin and candidate drivers of G4-MB, and to develop pre-clinical mouse models that reflect G4-MB tumorigenesis. We have developed a tumor mouse model that allows us to manipulate early iPSC-derived neuroepithelial stem cells, a cell population suggested as the cell-of-origin for but not limited to G4-MB. Using this model we have shown that the G4-MB candidate drivers SRC and ERBB4 induce tumor formation in *TP53^{WT}* and *TP53^{mut}* NESCs. Furthermore we are testing pre-clinical therapies of SRC inhibition in our SRC-ERBB4 tumor-bearing mice and are exploring other genetic G4-MB drivers such as ZMYM3. Our mouse models established here will decipher the yet unknown origin of Group 4 medulloblastoma and inform about basic principles of tumorigenesis in the brain.

15. SUBJECT TERMS

Pediatric Cancer; Medulloblastoma; Neuroepithelial Stem Cells; Tumorigenesis; SRC; ERBB4; ZMYM3

16. SECURITY CLASSIFICATION OF: U			17. LIMITATION OF ABSTRACT	18. NUMBER OF PAGES	19a. NAME OF RESPONSIBLE PERSON
a. REPORT	b. ABSTRACT	c. THIS PAGE			USAMRDC
U	U	U	UU	27	19b. TELEPHONE NUMBER *(include area code)*

Table of Contents

INTRODUCTION

Group 4 medulloblastoma (G4-MB) is the most common, yet least understood medulloblastoma subgroup: both in terms of driver pathways and cell-of-origin. Despite comprehensive genomic studies, G4-MB cases cannot be explained by known oncogenic drivers. On the molecular level great heterogeneity can be found within the G4-MB subgroup aggravating the understanding of G4-MB biology. G4-MBs show loss of *TP53*-mediated cell cycle checkpoint function, and alterations in chromatin modifiers such as loss-of-function mutations in *ZMYM3* contribute to approximately 30-40% of G4-MB patients. On the proteomic level increased receptor tyrosine kinase (RTK) signaling through activated ERBB4 and SRC has been suggested as a key player in G4-MB biology. However, it is unclear if these alterations represent actual drivers of G4-MB. Mouse models of G4-MB are not available, and the origin of G4-MB is still unclear. Development of targeted G4-MB therapies, which are currently completely lacking, will require identifying both cells-of-origin and drivers of G4-MB tumorigenesis. To test the role of hindbrain stem cells as the G4-MB cell-of-origin and identify key drivers in G4-MB tumorigenesis, we have established a xenograft model of human iPSC-derived neuroepithelial stem cells (NESC), a cell population showing dorsal hindbrain specification. We will use this model to analyze the potential oncogenic function of ERBB4 and SRC, and loss-of-function mutations in *ZMYM3* to form medulloblastoma *in vivo*. Furthermore, we will test potential drug targets of SRC-ERBB4 derived tumors *in vitro* and *in vivo* and analyze the molecular and cellular consequences of aberrant function of ZMYM3 in NESCs. This project will inform about basic principles of development and tumorigenesis in the brain. Expected results from our proposed project will further elucidate the molecular mechanisms in the origin of medulloblastoma and allow us to improve current treatment strategies for medulloblastoma.

KEYWORDS

Pediatric Cancer
Medulloblastoma
Neuroepithelial Stem Cells
Tumorigenesis
SRC
ERBB4
ZMYM3

ACCOMPLISHMENTS

What were the major goals of the project?

Major Goal/Task	Goal	Timeline (Months)	Percentage completed
1	Determine if SRC^{OE}/$ERBB4^{OE}$ signaling in human neuroepithelial stem cells causes G4-MB formation *in vivo*.	4-18	100%
2	Test whether targeted treatment with dasatinib in SRC^{OE}/$ERBB4^{OE}$ $TP53^{WT}$ and $TP53^{MUT}$ NES tumor-bearing mice prolongs survival.	6-20	100%
3	Originally: Introduce patient-derived ZMYM3 frameshift mutations P48Lfs*65 and R1111fs*9 into the genome of $TP53^{wt}$ and $TP53^{mut}$ human iPSC-derived NESCs. Alternative approach: Introduce patient-derived ZMYM3-Q322* overexpression in TP53wt and TP53mut human iPSC-derived NESCs.	4-16	50%
4	Originally: Determine if ZMYM3 frameshift mutations P48Lfs*65 and R1111fs*9 in $TP53^{wt}$ and $TP53^{mut}$ NESCs introduces tumor growth *in vivo.* Alternative approach: Determine if ZMYM3 Q3222* mutation in $TP53^{mut}$ NESCs induces tumor growth *in vivo.*	10-24	0%

What was accomplished under these goals?

Major Goal 1: Determine if SRC^{OE}/$ERBB4^{OE}$ signaling in human neuroepithelial stem cells causes G4-MB formation *in vivo*.

For Major Goal 1 of this proposal, we wanted to test if forced expression of SRC and ERBB4 in neuroepithelial stem cells (NESC) drives tumor formation *in vivo* and will generate tumors with a Group 4 medulloblastoma (G4-MB) signature.

For Subtask 1 under Major Goal 1 we tested if upregulated SRC and ERBB4 signaling in NESCs functions as tumor driver *in vivo*. Therefore, we overexpressed SRC and ERBB4 ($SRC^{OE}ERBB4^{OE}$) in $TP53^{mut}$ or $TP53^{wt}$ human NESCs via lentivirus transduction. If not otherwise stated, for all experiments described in Major Goal 1 $SRC^{OE}ERBB4^{OE}$;$TP53^{mut}$ NESCs and its controls (SRC^{OE};$TP53^{mut}$ NESCs, $ERBB4^{OE}$;$TP53^{mut}$ NESCs, and empty vector $TP53^{mut}$ NESCs or wild-type NSCs) were tested. We then determined tumorigenesis of SRC and ERBB4 overexpression NESCs by injection of 300,000 NES cells into the cerebellum of 6-8-week-old immunocompromised NOD-scid IL2Rgamma (NSG) mice with a group size n=10 for each NESC genotype (Fig. 1A). Mice were monitored for tumor growth with bioluminescence imaging for up

to one year after transplantation and euthanized when reaching humane endpoints or at 12 months after injection (Fig. 1B). We found that $SrcA^{OE}$ alone and $SrcA^{OE}$ with $ErbB4^{OE}$ in wild-type NESCs promotes tumor growth *in vivo* and mice reach endpoint around 60 days for $SrcA^{OE}$ alone and around 80 days with combination of $SrcA^{OE}$ and $ErbB4^{OE}$ (Fig. 1C). We see a 10% penetrance with slow tumor formation in $ErbB4^{OE}$ wild-type NESCs with one mouse at endpoint at 190 days, while all other mice in this group did not develop any tumors. In $TP53^{mut}$ NESCs we find slightly more aggressive tumor growth for $SrcA^{OE}$ alone with 40 days of average survival and 60 days average survival with combination of $SrcA^{OE}$ and $ErbB4^{OE}$ (Fig. 1E). As well for $ErbB4^{OE}$ alone we find a tumor penetrance of 10% (1 mouse) with a survival of 125 days, while all other mice in this group developed no tumors.

Developed tumors were dissected at endpoint. If tumors were visible and of reasonable size (> 2x2x2 mm) tumor tissue was subjected to standard histopathology such as Hematoxylin and Eosin (H&E) staining and immunohistochemistry for Ki67. H&E of coronal sections of the cerebellum show nuclear dense and non-infiltrative areas of tumor tissue with positivity for the cell proliferation marker Ki67 (Fig. 1D).

For Subtask 2 and 3 under Major Goal 1 we wanted to molecularly profile obtained tumors from Subtask 1 by DNA methylation and gene expression analysis and compare their profiles with human medulloblastoma samples to define G4-MB specificity. Tumor tissue was harvested from each tumor at endpoint and if visible and of reasonable size (> 2x2x2 mm) and snap frozen. Frozen tissues were subjected to DNA and RNA extraction and further genomic analyses. Tumor DNA

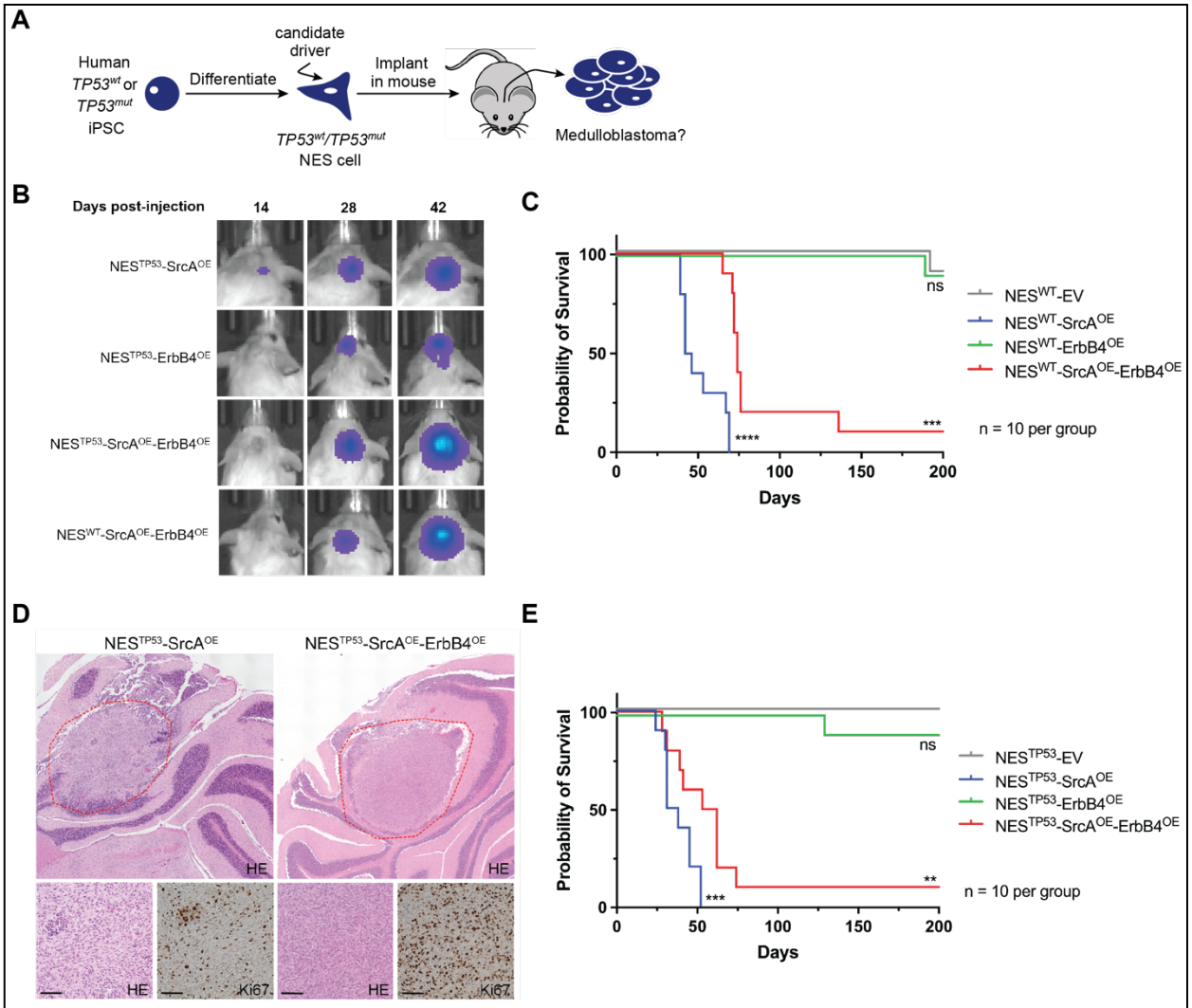

Figure 1. *In vivo* tumor formation of wild-type and TP53^{mut} NESCs with overexpression of Src or ErbB4. (A) Schematic of *in vivo* model using hiPSC-derived NESCs as an orthotopic xenograft to study tumor formation in mice. **(B)** Bioluminescence imaging of mice injected with TP53^{mut}-SrcA^{OE}, TP53^{mut}-ErbB4^{OE}, TP53^{mut}-SrcA^{OE}-ErbB4^{OE} and TP53^{WT}-SrcA^{OE}-ErbB4^{OE} NESCs**. (C)** Survival curve of mice injected with wildtype NESCs with SrcA or ErbB4 overexpression alone, or combination of SrcA and ErbB4. **(D)** HE and Ki67 immunohistochemistry of tumor sections derived from TP53^{mut}-SrcA^{OE} and TP53^{mut}-SrcA^{OE}-ErbB4^{OE} NESCs. Tumor areas are indicated with red dashed line. **(E)** Survival curve of mice injected with TP53^{mut} NESCs with SrcA or ErbB4 overexpression alone, or combination of SrcA and ErbB4. *EV = empty vector, NES^{TP53} refers to mutated TP53, scale bar = 100 µm, ns = not significant, ** = p<0.01, *** = p<0.001, **** = p<0.0001.*

was used for whole-genome bisulfite sequencing and DNA methylation clustering was performed using a methylation profiling classifier with a public reference cohort of over 2,800 neuropathological tumors of almost all known entities, including medulloblastoma. We subjected one SrcA^{OE} NES^{TP53mut}, three SrcA^{OE}-ErbB4^{OE} NES^{TP53mut} and three SrcA^{OE} NES^{TP53WT} tumors to

DNA methylation profiling. None of the tumors matched with any pediatric neuropathological tumors depicted by a low calibration score in the analysis (Table 1). While this result could be due to low quality of DNA content in our tumor samples and preparations, it is very unlikely. Most likely it shows that our obtained tumors do not resemble medulloblastoma or any other class of pediatric central nervous system tumors by DNA methylation.

Table 1. DNA methylation clustering in SrcA^{OE} and SrcA^{OE}-ErbB4^{OE} TP53^{WT} and TP53^{MUT} NESCs.

Sample	Calibration Score*	Match
NES^{TP53mut}-SrcA^{OE}-1	0.34	no
NES^{TP53mut}-SrcA^{OE}-ErbB4^{OE}-1	0.55	no
NES^{TP53mut}-SrcA^{OE}-ErbB4^{OE}-2	0.6	no
NES^{TP53mut}-SrcA^{OE}-ErbB4^{OE}-3	0.51	no
NES^{TP53WT}-SrcA^{OE}-1	0.45	no
NES^{TP53WT}-SrcA^{OE}-2	0.44	no
NES^{TP53WT}-SrcA^{OE}-3	na	no

* Probability that measure the confidence in the class assignment.
Score >= 0.9 is defined as a match with high confidence. Score < 0.9 is defined as no match.

For gene expression profiling of the obtained tumors we isolated RNA from three SrcA^{OE} NES^{TP53mut}, three SrcA^{OE}-ErbB4^{OE} NES^{TP53mut} and three SrcA^{OE} NES^{TP53WT} and ran RNA sequencing and downstream analysis on the obtained data.

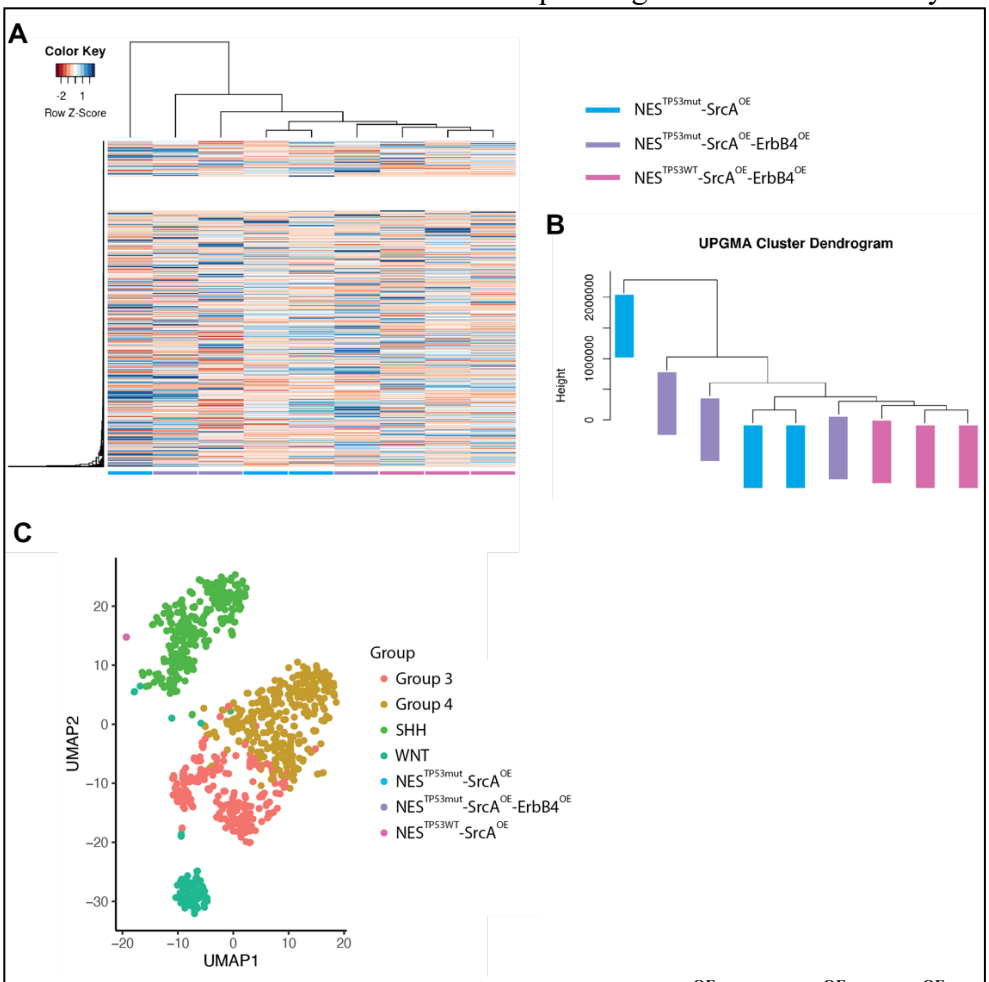

Figure 2. RNA sequencing and gene expression profiling of SrcA^{OE} and SrcA^{OE}-ErbB4^{OE} in TP53^{WT} and TP53^{mut} NESCs. Heat map **(A)** and cluster dendogram **(B)** of hierarchical clustering of NES^{TP53mut}-SrcA^{OE}, NES^{TP53mut}-SrcA^{OE}-ErbB4^{OE} and NES^{TP53WT}-SrcA^{OE}-ErbB4^{OE} tumor gene expression analysis. **(C)** Gene expression profiling of NES^{TP53mut}-SrcA^{OE}, NES^{TP53mut}-SrcA^{OE}-ErbB4^{OE} and NES^{TP53WT}-SrcA^{OE}-ErbB4^{OE} tumors and human medulloblastoma primary tumor samples using UMAP clustering.

We performed gene expression clustering of our Src-ErbB4 tumors among them and among medulloblastoma patient samples. We find that the SrcA^{OE} NES^{TP53mut} and SrcA^{OE}-ErbB4^{OE} NES^{TP53mut} cluster close together while the SrcA^{OE}-ErbB4^{OE} NES^{TP53WT} tumors form their own separate cluster (Fig. 2A and 3B). When clustering our tumor samples with gene expression data of medulloblastoma samples across all subgroups we find that our Src-ErbB4 do not cluster close to any of the subgroups and lie closest to the sonic hedgehog (SSH) medulloblastoma (Fig. 2C). Most surprisingly in this analysis all our Src-ErbB4

tumors cluster very tightly together, which needs to be further investigated to rule out technical issues with the data analysis.

Major Goal 2: Test whether targeted treatment with Dasatinib in SRC^{OE}/ERBB4^{OE} TP53^{WT} and TP53^{MUT} NES tumor-bearing mice prolongs survival.

For Major Goal 2 of this proposal we wanted to test whether targeted treatment strategies against Src pathway activation *in vitro* and *in vivo* will prolong survival of SrcA^{OE} and SrcA^{OE}-ErbB4^{OE} tumor mice.

To test whether *TP53^{MUT}* SrcA^{OE} and *TP53^{MUT}* SrcA^{OE}-ErbB4^{OE} NESCs are sensitive to targeted treatment against Src and receptor tyrosine kinase pathway activity we treated cells with the Src inhibitors Dasatinib and Tirbanibulin *in vitro* and subsequently treat tumor-bearing mice with Dasatinib. *In vitro* we find high sensitivity of *TP53^{MUT}* SrcA^{OE} and *TP53^{MUT}* SrcA^{OE}-ErbB4^{OE} NESCs against both inhibitors with an IC50 of 18-25 nM for Tirbanibulin (**Figure 3A**) and an IC50 of 5-11 nM for Dasatinib (**Figure 3B**) 72 hours after treatment. We found the highest sensitivity for Dasatinib in *TP53^{MUT}* SrcA^{OE} NESCs.

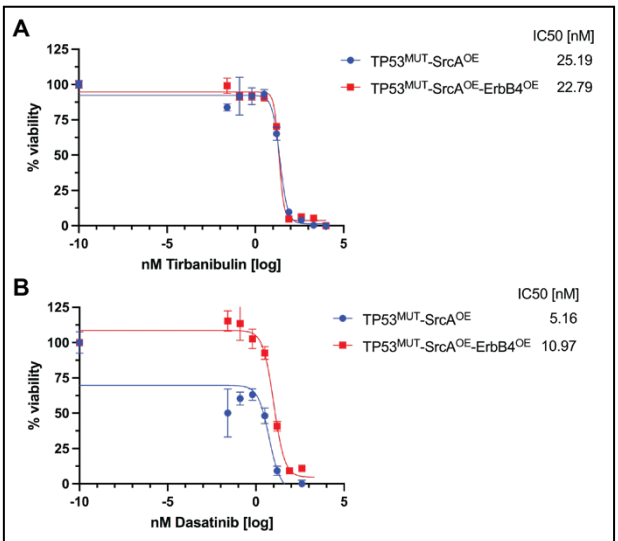

Figure 3. IC50 curves of Src inhibitors in TP53^{MUT}-SrcA^{OE} and TP53^{MUT}-ScrA^{OE}-ErbB4^{OE} NESCs. (A) Tirbanibulin IC50 curve in *TP53^{MUT}* SrcA^{OE} and *TP53^{MUT}* ScrA^{OE}-ErbB4^{OE} NESCs. (B) Dasatinib IC50 curve in *TP53^{MUT}* SrcA^{OE} and *TP53^{MUT}* ScrA^{OE}-ErbB4^{OE} NESCs.

Furthermore, we tested Dasatinib treatment in *TP53^{MUT}* SrcA^{OE} and *TP53^{MUT}* SrcA^{OE}-ErbB4^{OE} tumor-bearing mice for reduced tumor growth and prolonged survival. This compound has been suggested to cross the blood-brain barrier in adults and children and is currently tested in several clinical trials for leukemia and two trials for pediatric brain cancer (NCT02015728, NCT02596828). Mice were randomly enrolled into the vehicle and dasatinib treatment arms (n=5 mice per treatment and NESC genotype) 14 days after NESC transplantation. Treatment was performed from Day 38 – 68 (30 days duration) with 20 mg/kg Dasatinib doses 3x/week via oral gavage. Tumor growth was monitored with weekly bioluminescence imaging. Mice were monitored for body weight and adverse effects to Dasatinib treatment. With a group size of n = 5 mice per treatment condition we found no significant changes in survival for both cohorts, *TP53^{MUT}* SrcA^{OE} (**Figure 4A**) and *TP53^{MUT}* SrcA^{OE}-ErbB4^{OE} NESC tumor-bearing mice (**Figure 4B**), compared to vehicle treatment. In terms of tumor growth we also find no significant change between dasatinib and vehicle treatment in both cohorts, *TP53^{MUT}* SrcA^{OE} (**Figure 4C,E**) and *TP53^{MUT}* SrcA^{OE}-ErbB4^{OE} (**Figure 4D,F**) tumor-bearing mice. We also performed immunohistochemistry on the tumor sections for the proliferation marker Ki-67 and apoptotic marker Cleaved Caspase 3 to determine changes in proliferation and cell death with dasatinib treatment. We could not find any changes in number of proliferative cells and apoptotic cells in tumor tissue among vehicle and dasatinib treatment (data not shown). Future steps outside of this funding period will include increasing the group size by repeating the dasatinib and vehicle treatment in n = 5 mice for each condition to get a clearer result and a higher power of confidence for the statistical analyses of the in vivo results.

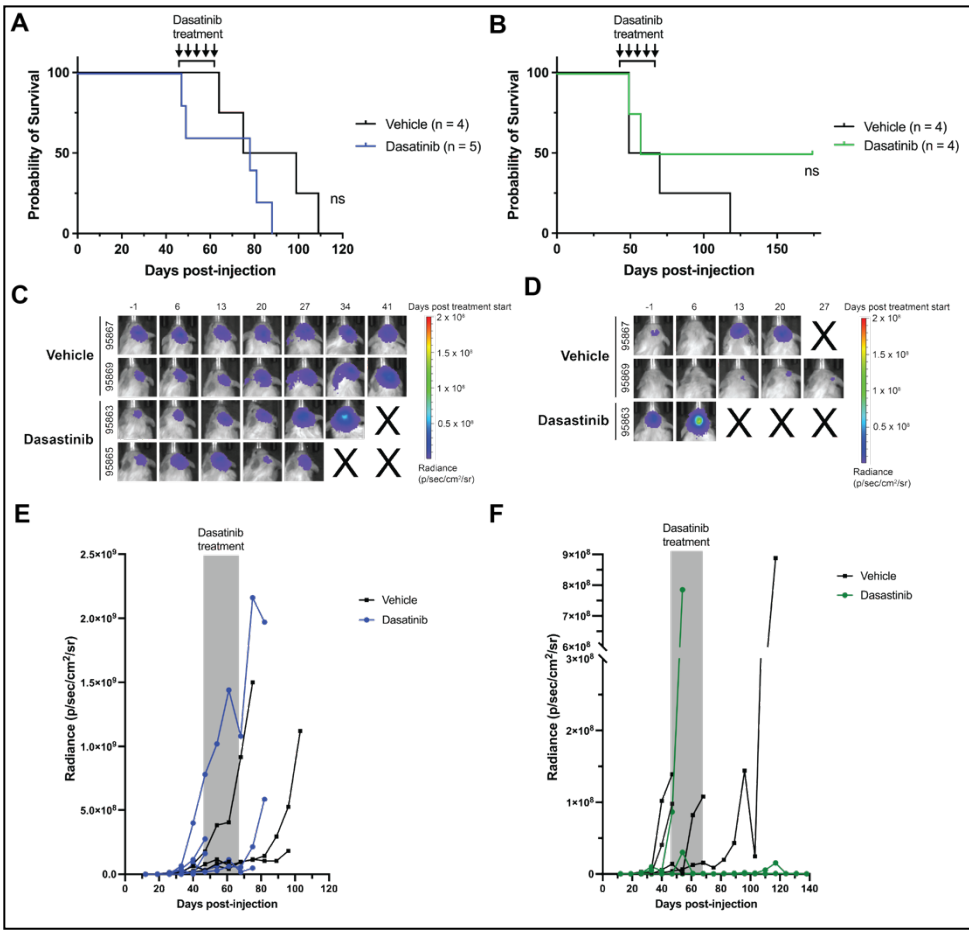

Figure 4. Dasatinib in vivo treatment in TP53^{MUT}-SrcA^{OE} and TP53^{MUT}-SrcA^{OE}-ErbB4^{OE} tumor-bearing mice. (A) Survival curve of TP53^{MUT}-SrcA^{OE} NESC tumor-bearing mice under Dasatinib treatment**. (B)** Survival curve of TP53^{MUT}-SrcA^{OE}-ErbB4^{OE} tumor-bearing mice under Dasatinib treatment. **(C, D)** Bioluminescence images of selected TP53^{MUT}-SrcA^{OE} and TP53^{MUT}-SrcA^{OE}-ErbB4^{OE} tumor-bearing mice respectively under vehicle and Dasatinib treatment. **(E,F)** Bioluminescence signal of TP53^{MUT}-SrcA^{OE} and TP53^{MUT}-SrcA^{OE}-ErbB4^{OE} tumor-bearing mice respectively under vehicle and Dasatinib treatment.

In summary for Major Goal 1 and 2 we could show that Src alone and in combination with ErbB4 induces tumor growth in NESCs, and cells *in vitro* are sensitive to targeted treatment of Src and receptor tyrosine kinase pathway inhibition. *In vivo* feasibility of Src inhibition in Src and ErbB4 NESC tumors has to be further determined with increased *in vivo* group sizes and adjustment of dosing of Dasatinib.

Major Goal 3: Determine if mutations in *ZMYM3* drive Group 4 medulloblastoma formation in human neuroepithelial stem cells *in vivo*.

For Major Goal 3 of this proposal we planned to introduce the patient-derived ZMYM3 frameshift mutations P48Lfs*65 and R1111fs*9 into the genome of TP53^{wt} and TP53^{mut} human iPSC-derived NESCs and study their tumorigenic potential *in vivo*.

For Subtask 1 under Major Goal 3 we planned to knockout endogenousZMYM3 in our human iPSCs (TP53 wildtype and TP53 mutated), differentiate them into NESCs and introduce the expression of P48Lfs*65 and R1111fs*9 *ZMYM3* mutations via lentiviral transduction (**Figure 5A**). For our knockout experiments we designed sgRNAs targeting the exon 2 locus of ZMYM3 and introduced the sgRNA-Cas9 ribonucleoprotein complex via nucleofection into hiPSCs. We designed two sgRNAs both targeting exon 2 of ZMYM3 and tested single sgRNA-Cas9 and combination sgRNA-Cas9 nucleofection to introduce larger deletions (**Figure 5B**). To analyze the size of our induced deletions we designed a PCR primer pair flanking both sgRNAs in exon 2 and generating a 1 kb PCR product in wildtype ZMYM3. We initially tested the efficiency of our nucleofection using a control GFP plasmid and find most hiPSCs GFP-positive 48 hours after transfection (**Figure 5C**). To test the efficiency of our sgRNA-Cas9 we nucleofected cells with single and combination of both sgRNAs, and harvested cells for genomic DNA isolation 7 days later. When running the PCR covering both sgRNAs, from here on referred as 'exon 2 PCR', we find only 1 kb products in the single sgRNA conditions, while combination of both sgRNAs also shows a PCR band at around 850 bp indication a local deletion in some of the cells (**Figure 5D**).

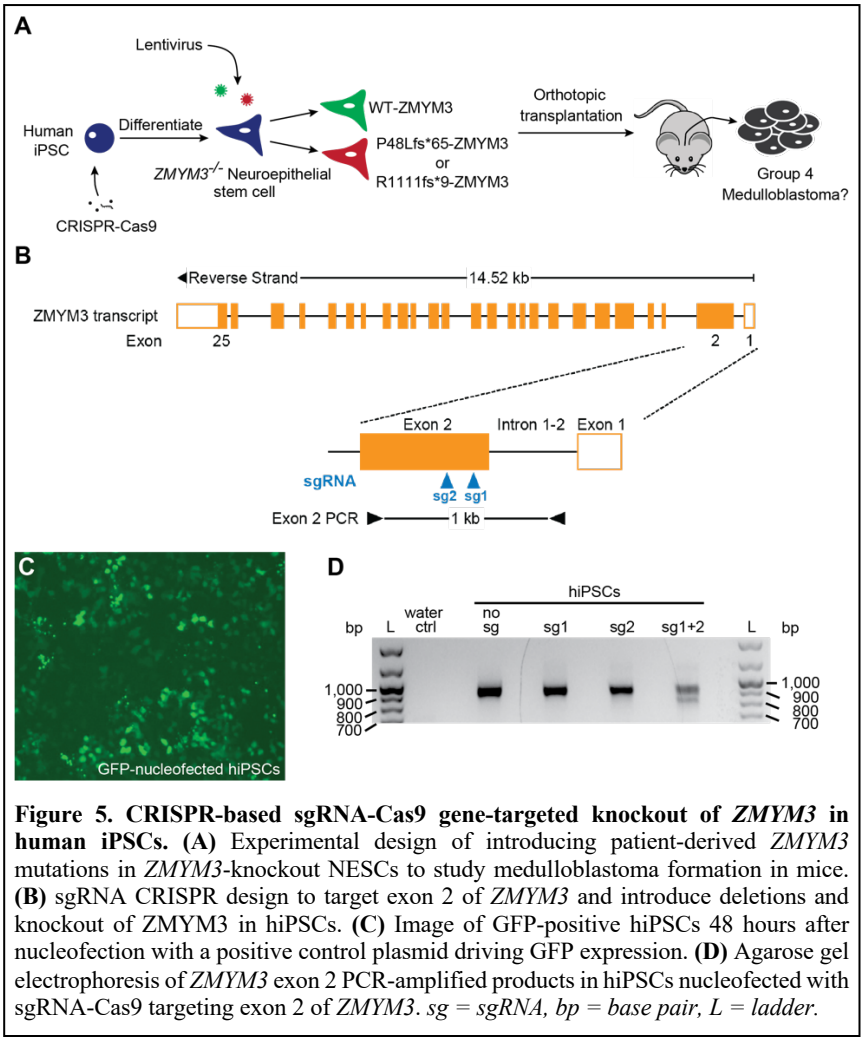

Figure 5. CRISPR-based sgRNA-Cas9 gene-targeted knockout of *ZMYM3* in human iPSCs. (A) Experimental design of introducing patient-derived *ZMYM3* mutations in *ZMYM3*-knockout NESCs to study medulloblastoma formation in mice. **(B)** sgRNA CRISPR design to target exon 2 of *ZMYM3* and introduce deletions and knockout of ZMYM3 in hiPSCs. **(C)** Image of GFP-positive hiPSCs 48 hours after nucleofection with a positive control plasmid driving GFP expression. **(D)** Agarose gel electrophoresis of *ZMYM3* exon 2 PCR-amplified products in hiPSCs nucleofected with sgRNA-Cas9 targeting exon 2 of *ZMYM3*. *sg = sgRNA, bp = base pair, L = ladder.*

To generate single-cell clones with a sgRNA-Cas9 induced deletion in ZMYM3 we nucleofected hiPSCs with both our sgRNAs and plated single cells in 96-well plates 48 hours after

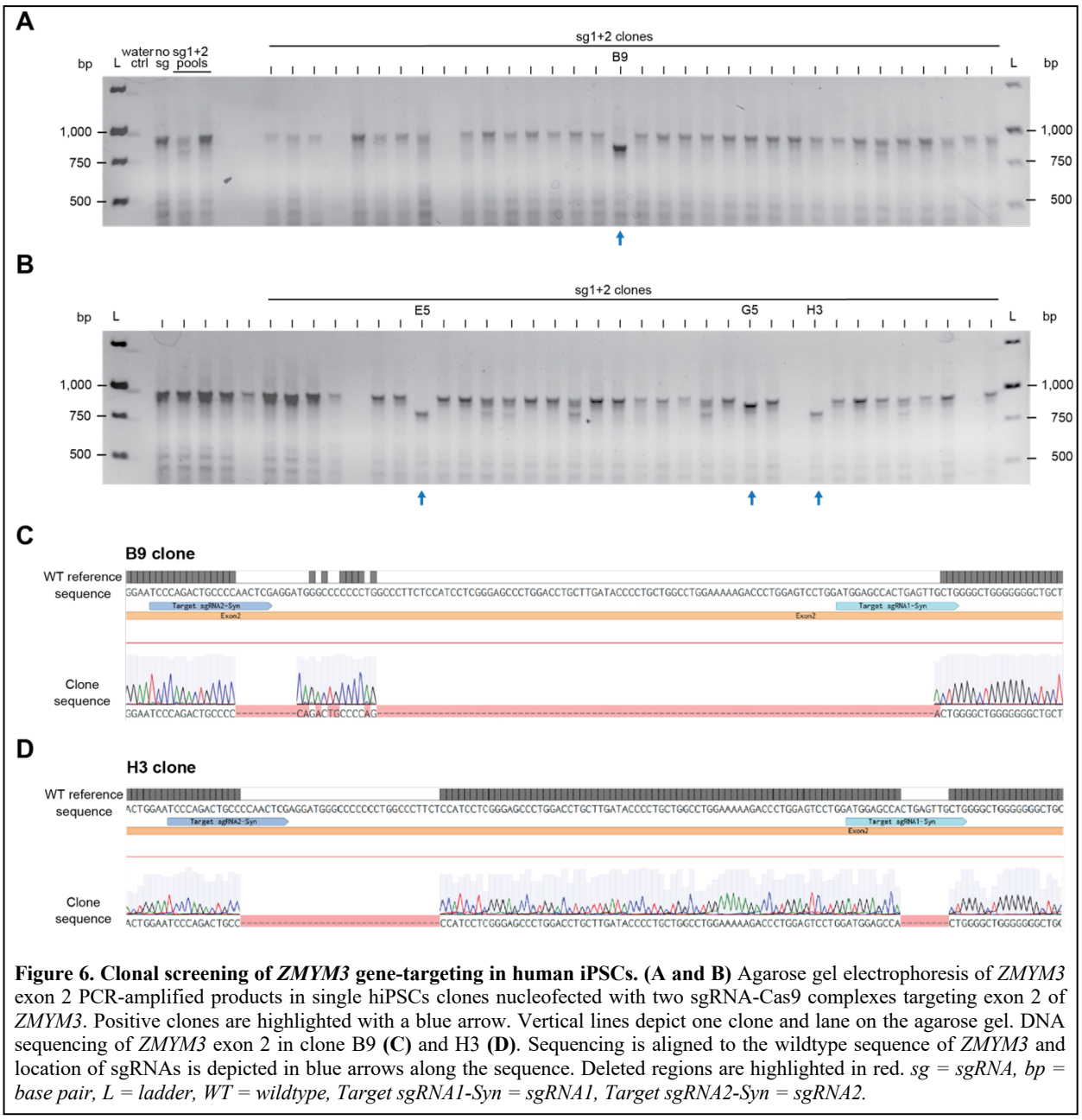

Figure 6. Clonal screening of *ZMYM3* gene-targeting in human iPSCs. (A and B) Agarose gel electrophoresis of *ZMYM3* exon 2 PCR-amplified products in single hiPSCs clones nucleofected with two sgRNA-Cas9 complexes targeting exon 2 of *ZMYM3*. Positive clones are highlighted with a blue arrow. Vertical lines depict one clone and lane on the agarose gel. DNA sequencing of *ZMYM3* exon 2 in clone B9 **(C)** and H3 **(D)**. Sequencing is aligned to the wildtype sequence of *ZMYM3* and location of sgRNAs is depicted in blue arrows along the sequence. Deleted regions are highlighted in red. *sg = sgRNA, bp = base pair, L = ladder, WT = wildtype, Target sgRNA1-Syn = sgRNA1, Target sgRNA2-Syn = sgRNA2.*

nucleofection. We grew up single-cell clones and harvested genomic DNA from a total of 74 clones for Exon 2 PCR screening for deletions in exon 2 of ZMYM3. For selection of positive clones we considered the Exon 2 PCR to show no band at 1 kb (wildtype size) but a smaller band visible on the gel. For the 74 screened clones we found 4 positive clones with a PCR band at around 800 bp instead of 1 kb (**Figure 6A and B**). Among the 74 screened clones we also found clones with a PCR band below 1 kb and with the wildtype 1kb band. This indicates that the clone came from several cells where some were wildtype and some acquired sgRNA-directed cuts in exon 2. We decided to move forward with the clones showing no wildtype 1 kb band anymore and sequenced the cut regions in exon 2 of ZMYM3 for clone B9 and H3. Clone E5 and G5

unfortunately started to differentiate in culture and therefore were excluded from further analysis and experiments. Clone B9 and H3 showed deleted regions of about 80 bp and 30 bp for the latter clone (**Figure 6C and D**).

To understand if the introduced cuts in exon 2 of ZMYM3 will lead to early termination of ZMYM3 transcription and loss of ZMYM3 on the protein level we first performed immunoblot and qRT-PCR analysis in the B9 and H3 clones. On protein level we do not see a knockout or knockdown of *ZMYM3* for both clones compared to wildtype cells (**Figure 7A**). For qRT-PCR analysis we designed two primer sets, one primer pair spanning exon 3 to 5 to determine expression levels right after the cut in exon 2, and one primer pair spanning exon 22 to 23 in order to determine expression levels of the 3'end of the full-length *ZMYM3* transcript. We find both regions of *ZMYM3* expressed in both clones indicating that *ZMYM3* mRNA is still being expressed in the cells (**Figure 7B**). Furthermore, we also sequenced the expressed transcript of ZMYM3 in the B9 clone by sequencing the reverse transcript generated from mRNA expression. We find that *ZMYM3* in the B9 clone is expressed and still harbors the deletions found in exon 2 through our gene-targeting (**Figure 7C**). Despite the introduced frameshift and around 80 bp deletion in exon 2 we find full-length *ZMYM3* mRNA being transcribed in the cells (full sequencing data not shown). This led us to the conclusion that we were not able to generate a gene-edited knockout or significant knockdown of *ZMYM3* and instead might have introduced a truncated version of ZMYM3. To verify our hypothesis, we generated protein transcripts based on our mRNA sequencing results and find that though the deletion in clone B9 introduces an early stop codon at amino acid 53, it also allows for an alternative start site at amino acid 230 that will span protein translation until the C-terminal end of ZMYM3. We therefore conclude that we most likely have generated a N-terminal truncated version of ZMYM3 in our clone that still expresses the functional domains in ZMYM3 and therefore will not be of use for this proposal. In order to reach our goals in this proposal we decided to skip the generation of *ZMYM3* knockout iPSCs and directly overexpress patient-derived *ZMYM3* mutations in our wildtype NESCs via lentiviral infection and conclude with our planned downstream experiments. This alternative approach was approved with the previous progress report and details and results are described below.

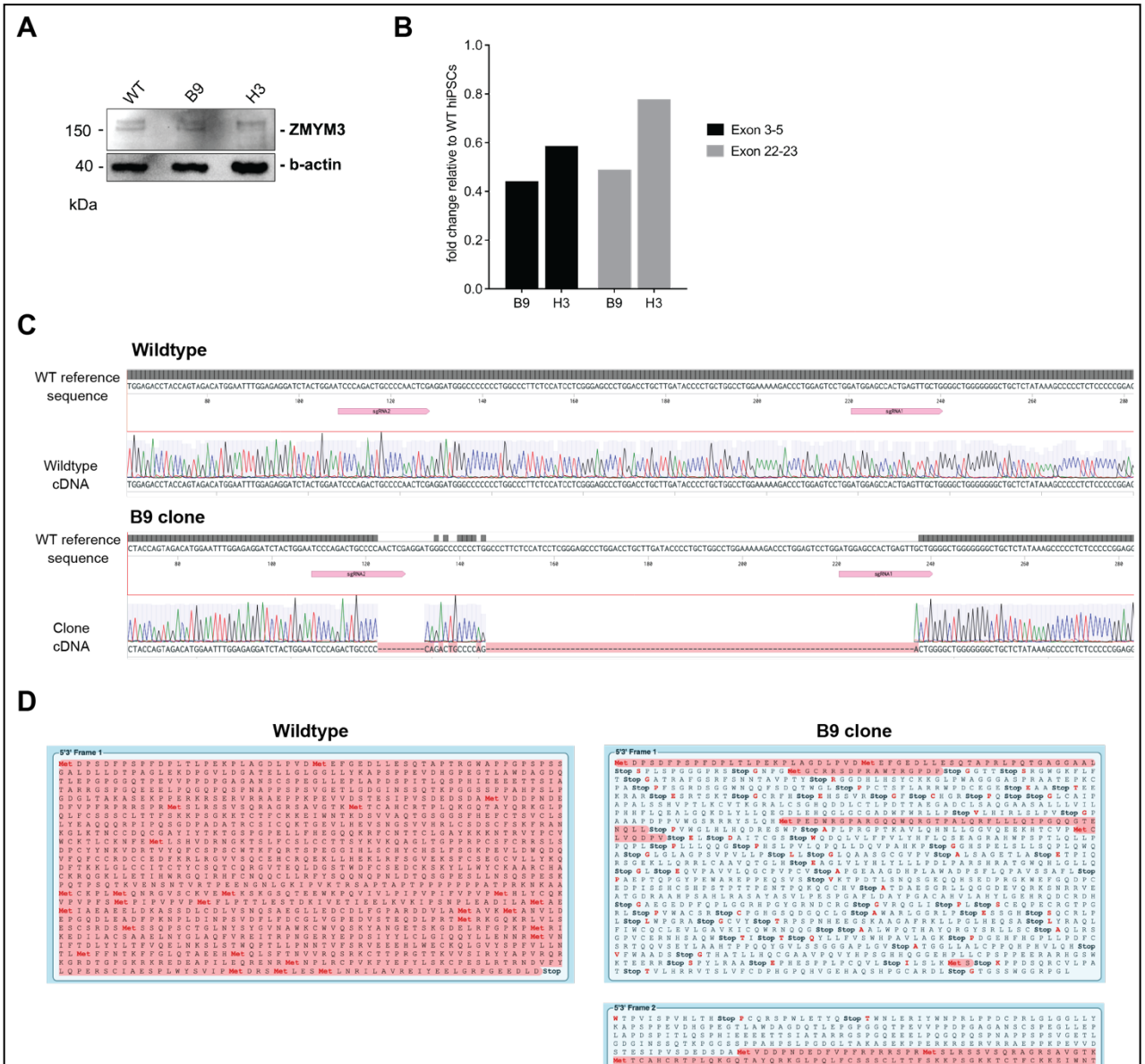

Figure 7. Downstream analysis of *ZMYM3* knockout in B9 and H3 clones. (A) Immunoblotting *ZMYM3* in wildtype and gene-targeted clones B9 and H3. **(B)** Quantitative real-time PCR of *ZMYM3* in iPSC clones B9 and H3. Primers were designed spanning exon 3 to 5 (Exon 3-5) and exon 22 to 23 (Exon 22-23). mRNA expression levels depict fold change to wildtype hiPSCs. **(C)** cDNA sequencing of *ZMYM3* exon 2 in wildtype hiPSCs and B9 clone. Sequencing is aligned to the wildtype sequence of *ZMYM3* and location of sgRNAs is depicted in pink arrows along the sequence. Deleted regions are highlighted in red. **(D)** Protein translation of wildtype *ZMYM3* sequence and B9 *ZMYM3* sequence based on the cDNA sequencing results. Protein translation and predicted protein transcripts were generated using Basic Local Alignment Search Tool (BLAST, website: https://blast.ncbi.nlm.nih.gov/Blast.cgi). Protein start sites are highlighted as 'Met' in red bold font, predicted protein sequence frames are highlighted in red. *WT = wildtype.*

Alternative Approach for Major Goal 3: Determine if overexpression of the Q322* mutation in ZMYM3 wildtype NESCs drives Group 4 medulloblastoma formation *in vivo*.

As an alternative approach for Major Goal 3 and in order to move along with introducing the ZMYM3 frameshift mutations in our neuroepithelial stem cells, we proposed in the previous progress report (September 2021) to skip knocking out endogenous ZMYM3 and go ahead with overexpressing ZMYM3 frameshift mutations with lentivirus in wildtype neuroepithelial stem cells (with persisting low levels of endogenous ZMYM3 (**Figure 8A, D**).

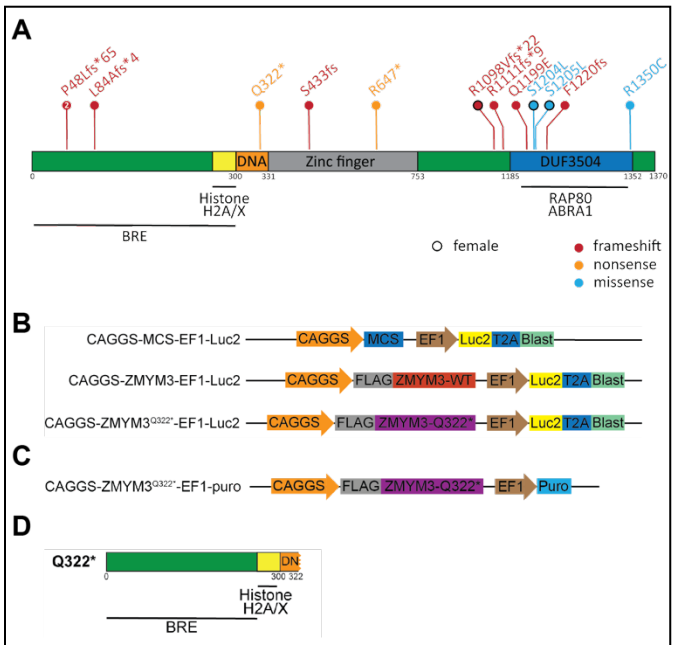

Figure 8. Schematics for alternative approach for Major Goal 3 and 4. (A) Schematic of human ZMYM3 functional domains and associated mutations found in Group 4 medulloblastoma. **(B,C)** Lentiviral constructs to introduce wildtype (CAGGS-ZMYM3-EF1-Luc2) and ZMYM3^{Q322*} (CAGGS-ZMYM3^{Q332*}-EF1-Luc2 and CAGGS-ZMYM3^{Q332*}-EF1-puro) overexpression in mammalian cells. **(D)** Schematic of truncated version of Q322* mutated ZMYM3.

For the revised Subtask 1 under Major Goal 3 we aimed to generate a lentiviral plasmid overexpressing the Q322* mutation of flag-tagged ZMYM3 and transduce our NESCs with this construct. This mutation as well depletes the active domains of ZMYM3 and disrupts the DNA binding domain, as well as the proposed DNA repair activity of ZMYM3 (**Figure 8D**). This will have no effects on the hypothesis, experimental approach and expected outcome of our study.

We generated two versions of this construct, one with a second promotor driving Luciferase and Blasticidin expression (for *in vivo* imaging and *in vitro* selection of transduced cells, respectively) and another. construct with a second promoter driving solely Puromycin expression for *in vitro* selection (**Figure 8B,C**). Control vectors were generated including wildtype flag-tagged- expression of ZMYM3 and empty vector version of this construct (**Figure 8B**).

Q322* mutation in ZMYM3 was introduced by targeted mutagenesis in the CAGGS-ZMYM3-EF1-Luc2 plasmid expressing wildtype ZMYM3. Expression of Q322* in the ZMYM3 transcript was confirmed by Sanger sequencing (**Figure 9A**). To confirm expression of ZMYM3-Q322* in our construct we transfected the human cell line 293T with wildtype ZMYM3 (ZMYM3-WT, CAGGS-ZMYM3-EF1-Luc2) and Q322* mutated ZMYM3 (ZMYM3-Q322*, CAGGS-ZMYM3^{Q322*}-EF1-Luc2) and performed immunoblotting against ZMYM3 and flag-tag. We could confirm expression of wildtype ZMYM3 with antibodies raised against ZMYM3 itself and flag-tag, as well as expression of a smaller ZMYM3^{Q322*} product using flag-tag (**Figure 9B**). Both proteins run at expected sizes (around 170 kDa for ZMYM3-WT, 70-75 kDa for ZMYM3$^{Q322*)}$ and we therefore conclude the successful expression of our genes of interest.

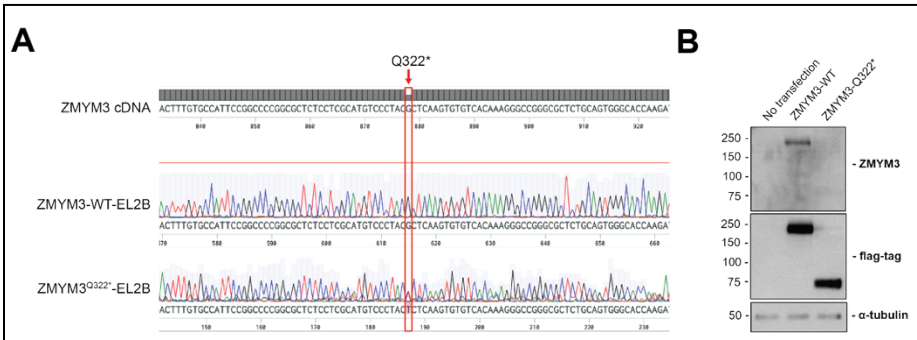

Figure 9. Generation of a mutant ZMYM3^{Q322*} overexpressing construct. (A) Sequencing traces of ZMYM3-WT-EL2B (wildtype ZMYM3) plasmid and ZMYM3^{Q322*}-EL2B construct. Q322* mutation is highlighted with a red box and arrow. **(B)** Immunoblot for ZMYM3 and flag-tag of 293T human fibroblasts transfected with the ZMYM3-WT and ZMYM3^{Q322*} plasmids.

To understand the role of ZMYM3^{Q322*} mutation in neural epithelial stem cells and Group 4 medulloblastoma formation we next transduced the NESCs with lentivirus overexpressing our generated ZMYM3-wildtype and ZMYM3^{Q322*} constructs. In the first round of lentiviral transductions we focused on the blasticidin constructs. Cells were selected under blasticidin and harvested for qRT-PCR to confirm expression of ZMYM3-WT and ZMYM3^{Q322*} . We designed two qRT-PCR primer pairs to detect the exon-exon junctions across exon 3-5 of ZMYM3 and the exon-exon junctions of exon 22-23 of ZMYM3. Exons 3-5 occur right before the location of the Q322* mutation and exon junction 22-23 is downstream of the mutation near the N-terminal end. We should see equal levels of expression for both primers, but significant increase in expression of both compared to empty vector NESCs (EV NESCs). Unfortunately, we do not find an increase in expression of both exon regions relative to EV NESCs (**Figure 10A**). To test if blasticidin selection in our system does not work well and cells become resistant to the selection, we repeated this experiment using the ZMYM3^{Q322*} blasticidin construct and compared it to the ZMYM3^{Q322*} puromycin construct in our NESCs. After transduction and selection of cells we harvested cells for immunoblotting against flag-tag and ZMYM3, respectively (**Figure 10B,C**). As control samples we also ran non-transfected NESCs, ZMYM3 wildtype NESCs and for flag-tag we added a flag-tagged MYCN transfected NESC sample. We find no overexpression of flag-tag in our ZMYM3 samples or MYCN positive control. Expected sizes are marked with a red arrow (**Figure 10B**). We have also tested different available flag-tag antibodies to rule out any issues with this specific antibody but could not find any improvements (data not shown). We additionally immunoblotted for ZMYM3 and could not find strong overexpression of ZMYM3 at least in the

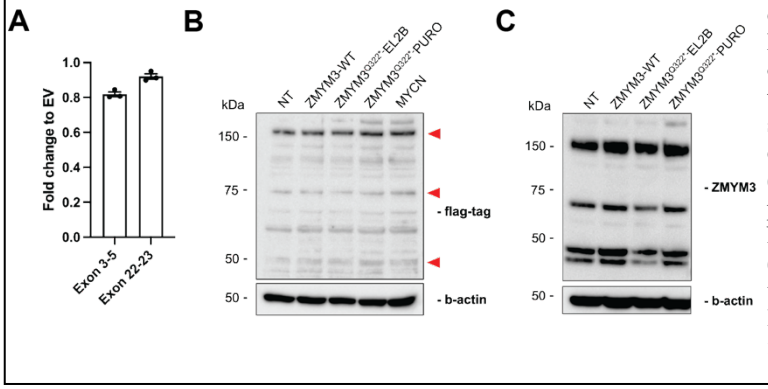

Figure 10. Validation of ZMYM3^{Q322*} overexpression in human NESCs. (A) qRT-PCR for ZMYM3 in ZMYM3Q322* overexpressing NESCs. Primers were designed to span the exon 3-5 and exon 22-23 of ZMYM3 sequence. **(B)** Immunoblot for flag-tag in NESCs either transduced with wildtype ZMYM3 (ZMYM3-WT), ZMYM3^{Q322*} or MYCN as a positive control. **(C)** Immunoblot for ZMYM3 in NESCs either transduced with wildtype ZMYM3 (ZMYM3-WT) or ZMYM3^{Q322*} . EV = empty vector, NT = no transfection, WT = wildtype; Red arrows show expected sizes for the fusion flag-tagged proteins.

ZMYM3 wildtype lane or a shortened ZMYM3^{Q322*} form at around 75 kDa for our mutation constructs (**Figure 10C**). In fact our ZMYM3 antibody gives us high background of unspecific bands, which we were not able to resolve until this point. To this end we have troubleshooted the generation of ZMYM3^{Q322*} NESCs by testing the following things: (1) We have sequenced the plasmids (CAGGS-ZMYM3-EF1-Luc2, CAGGS-ZMYM3^{Q322*}-EF1-Luc2-Blast, CAGGS-ZMYM3^{Q322*}-EF1-Puro) entirely to rule out any spontaneous mutations or recombinations that could have occurred during cloning, DNA preparations and lentiviral preparation. No issues were found (data not shown). (2) We have performed test transfection and lentiviral transductions with all constructs in 293T cells (since they are easy to transfect/transduce with high efficiency), have selected lentivirus transduced cells with either blasticidin and puromycin and re-run immunoblotting. (3) For immunoblotting we tried out different flag-tag and ZMYM3 antibodies in NESCs and 293T cells. We still could not see a signal for flag-tag or overexpression of ZMYM3 or Q322* mutations in the respective conditions (data not shown).

For revised Subtask 2 under Major Goal 3 we were planning to determine whether *ZMYM3-322** mutation in NESCs induces a proliferative advantage *in vitro* and regulates DNA repair responses after introducing DNA double-strand breaks in cells. Subtask 2 of Major Goal 3 was planned to be accomplished in Year 1-2 (Months 10-16), but due to the delays in accomplishing Subtask 1 of Major Goal 3 Subtask 2 of Major Goal 3 could not be accomplished within the time frame of this funded project.

Revised Major Goal 4: Determine if ZMYM3 mutation 322* in TP53^{wt} and TP53^{mut} NESCs introduces tumor growth *in vivo*.

For revised Major Goal 4 of this proposal we were planning to determine the tumorigenic effect of *ZMYM3-Q322** mutation *in vivo* and perform DNA methylation and gene expression profiling analyses of obtained tumors. Major Goal 4 was planned to be accomplished in Year 2 (Months 12-24) of this proposal, but due to the delays in accomplishing Subtask 1 of Major Goal 3 Major Goal 4 could not be accomplished within the time frame of this funded project.

In summary, while we were not able to accomplish functional studies with ZMYM3 mutations in NESCs yet, we were able to generate overexpressing constructs of ZMYM3-Q322* to study its function in neural stem cells and medulloblastoma formation.

What opportunities for training and professional development has the project provided?

As the Principal Investigator of this proposal I have received individual training from both my mentors Dr. William Weiss and Dr. Bjoern Schwer in weekly one-on-one meetings, bi-monthly progress discussion meetings with Dr. Weiss and Dr. Schwer together, and I have presented and discussed this work in our group meetings in both laboratories every 3 months. During all those meetings the progress of the project was discussed in detail and I received mentorship and expertise advice for troubleshooting certain parts of this project. I have also presented and discussed this work with our collaboration partner for this project Dr. Michael D. Taylor and his laboratory and we have discussed the objectives and outcomes of the bioinformatical data analysis. This has increased my knowledge and critical thinking when it comes to data analysis and genomic analyses and will help me to become more skilled in this field.

Due to the COVID19 pandemic in Year 1 and Year 2 of this funding period it was not possible for me to attend professional meetings or research conferences to present my work and discuss my work with peers in my research field. Meanwhile to improve my skills in bioinformatics and data analysis of genomic datasets, such as RNA-seq and gene expression arrays, I have participated in a one-week virtual workshop for RNA-seq data analysis hosted by the Bioinformatics Core of the University of California Davis in June 2021. This has allowed me to analyze some of the RNA-seq data we have obtained in this proposal and become more skilled with our sequencing data analysis.

How were the results disseminated to communities of interest?
Nothing to Report.

What do you plan to do during the next reporting period to accomplish the goals?
Nothing to Report.

IMPACT

What was the impact on the development of the principal discipline(s) of the project?
Subgroup 4 of medulloblastoma is a childhood brain cancer that is poorly understood and lacks specific and successful treatment strategies. With the here funded project we aimed to understand the genetic events leading to formation of these tumors and to test potential targeted drug treatment therapies pre-clinically in mice. In particular we have found that activation of the receptor tyrosine kinase pathway via the regulators Src and ErbB4 in neuroepithelial stem cells induces tumor formation in mice. Furthermore we find that treatment of tumor-bearing mice with the Src inhibitor Dasatinib might slow down tumor growth. Further studies in mice are necessary to validate these results and will open up discussions about Src inhibitor treatment in children with Group 4 medulloblastoma with receptor tyrosine kinase activation.

What was the impact on other disciplines?
Nothing to report.

What was the impact on technology transfer?
Nothing to report.

What was the impact on society beyond science and technology?
Nothing to report.

CHANGES/PROBLEMS

Changes in approach and reasons for change

Nothing to report.

Actual or anticipated problems or delays and actions or plans to resolve them

Specific Aim 1 – Determine if aberrant SRC/ERBB4 signaling in human NESCs causes G4-MB formation *in vivo*. For Major Task 1 and 2 of Specific Aim 1 we were able to show that Src^{OE} alone and in combination with $ErbB4^{OE}$ induces tumor growth in NESCs, and cells *in vitro* are sensitive to targeted treatment of Src and receptor tyrosine kinase pathway inhibition. *In vivo* feasibility of Src inhibition with Dasatinib in Src^{OE} and $ErbB4^{OE}$ NESC tumors is so far inconclusive and has to be further determined with increased group sizes and adjustment of dosing of Dasatinib.

Specific Aim 2 – Determine if mutations in *ZMYM3* drive G4-MB formation in human NESCs. Unfortunately, we were not able to fully accomplish Specific Aim 2 of this proposal. For Major Task 1 of Specific Aim 2 we were unable to generate CRISPR-mediated ZMYM3 knockout NESCs in Year 1 of this funding. For Year 2 of the funding period we changed our approach to overexpress mutations of ZMYM3 via lentiviral transduction in NESCs expressing endogenous ZMYM3. While we were able to generate lentiviral particles and tested those in the NESCs, we could not find expression of mutant ZMYM3 on mRNA and protein level. Year 2 of the funding period was spent to generate those reagents, test them in NESCs and run troubleshooting experiments to figure out potential issues. Future directions will focus on further understanding the issue with our lentiviral particles to introduce overexpression of ZMYM3 mutations in NESCs.

Changes that had significant impact on expenditures.

Nothing to Report.

Significant changes in use or care of human subjects, vertebrate animals, biohazards, and/or select agents.

Nothing to Report.

Significant changes in use or care of human subjects.

Nothing to Report.

Significant changes in use or care of vertebrate animals.

Nothing to Report.

Significant changes in use of biohazards and/or select agents.

Nothing to Report.

PRODUCTS

Publications, conference papers, and presentations

- **Journal publications**
  Nothing to Report.

- **Books or other non-periodical, one-time publications**
  Nothing to Report.

- **Other publications, conference papers, and presentations**
  Nothing to Report.

Website(s) or other Internet site(s)
Nothing to Report.

Technologies or techniques
Nothing to Report.

Inventions, patent applications, and/or licenses
Nothing to Report.

Other Products

- **Data or databases**
  Nothing to Report.

- **Biospecimen collections**
  Nothing to Report.

- **Audio or video products**
  Nothing to Report.

- **Software**
  Nothing to Report.

- **Models**
  Nothing to Report.

- **Educational aids or curricula**
  Nothing to Report.

- **Instruments or equipment**
  Nothing to Report.

- **Research material**
  - Cell lines that were developed in Year 1 of this proposal:
    - SRC^{OE};$TP53^{WT}$ NESCs
    - $ERBB4^{OE}$;$TP53^{WT}$ NESCs
    - SRC^{OE}-$ERBB4^{OE}$;$TP53^{WT}$ NESCs
    - EV-$TP53^{WT}$ NESCs (empty vector)
    - SRC^{OE};$TP53^{mut}$ NESCs
    - $ERBB4^{OE}$;$TP53^{mut}$ NESCs
    - SRC^{OE}-$ERBB4^{OE}$;$TP53^{mut}$ NESCs
    - EV-$TP53^{mut}$ NESCs (empty vector)

- **Clinical interventions**
  Nothing to Report.

- **New business creation**
  Nothing to Report.

- **Other**
  Nothing to Report.

PARTICIPANTS & OTHER COLLABORATING ORGANIZATIONS

What individuals have worked on the project?

Name:	Christin Schmidt
Project Role:	PI
Researcher Identifier (e.g. ORCID ID):	0000-0002-2225-0583
Nearest person month worked:	24
Contribution to the Project:	Designed, performed and analyzed all the current experiments under this project.
Funding Support:	na

Has there been a change in the active other support of the PD/PI(s) or senior/key personnel since the last reporting period?

Nothing to Report.

What other organizations were involved as partners?

Organization Name	Michael D. Taylor Lab Division of Neurosurgery The Hospital for Sick Children
Location of Organization	686 Bay str. 17.9713 Toronto, Canada
Partner's contribution to the project	Bioinformatic analysis of DNA methylation and gene expression of obtained tumors in this project.

SPECIAL REPORTING REQUIREMENTS
Nothing to Report.

APPENDICES
Nothing to Report.